



Inhibition of *Escherichia coli* O157:H7 motility and biofilm by β -Sitosterol glucoside



Amit Vikram, G.K. Jayaprakasha, Ram M. Uckoo, Bhimanagouda S. Patil *

Vegetable and Fruit Improvement Center, Department of Horticultural Sciences, Texas A&M University, College Station, TX 77843, USA

ARTICLE INFO

Article history:

Received 26 December 2012

Received in revised form 1 July 2013

Accepted 19 July 2013

Available online 25 July 2013

Keywords:

Citrus

Phytosterol

Polymethoxyflavones

Anti-virulence

Flagella

RssAB

Hns

ABSTRACT

Background: *Escherichia coli* O157:H7 (EHEC) is a food borne pathogen, which causes diarrhea and hemolytic uremic syndrome (HUS). There is an urgent need of novel antimicrobials for treatment of EHEC as conventional antibiotics enhance shiga toxin production and potentiate morbidity and mortality.

Methods: Six bioactive compounds were isolated, identified from citrus and evaluated for the effect on EHEC biofilm and motility. To determine the possible mode of action, a series of genes known to affect biofilm and motility were overexpressed and the effect on biofilm/motility was assessed. Furthermore, the relative expression of genes involved in motility and biofilm formation was measured by qRT-PCR in presence and absence of phytochemicals, to examine the repression caused by test compounds.

Results: The β -sitosterol glucoside (SG) was identified as the most potent inhibitor of EHEC biofilm formation and motility without affecting the cell viability. Furthermore, SG appears to inhibit the biofilm and motility through *rssAB* and *hns* mediated repression of flagellar master operon *flhDC*.

Conclusion: SG may serve as novel lead compound for further development of anti-virulence drugs.

General significance: Plant sterols constitute significant part of diet and impart various health benefits. Here we present the first evidence that SG, a plant sterol has significant effect on EHEC motility, a critical virulence factor, and may have potential application as antivirulence strategy.

© 2013 Elsevier B.V. All rights reserved.

1. Introduction

Emergence of antibiotic resistance has produced substantial medical challenges and a sense of urgency to identify and develop novel antimicrobials [1]. In order to overcome the virulence of antibiotic resistant strains, novel targets are constantly being searched and identified. Efforts in laboratories across the globe have identified several processes and microbial structures such as type three secretion system, quorum sensing, host–pathogen interaction, efflux systems and bacterial membrane functions as significant targets for development of novel antimicrobials [1].

Enterohaemorrhagic *Escherichia coli* (EHEC) O157:H7 is a Gram-negative foodborne pathogen that causes bloody diarrhea. EHEC colonizes the large intestine and produces attaching and effacing (AE) lesions and Shiga toxin. EHEC and other Shiga toxin producing *E. coli* strains harbor the gene encoding the toxin on a lysogenic phage. Antibiotic treatment often results in phage induction and hyper-production of toxin, leading to fatal hemorrhagic colitis and hemolytic uremic syndrome [2]. Therefore, the treatment options for EHEC infections are limited to intravenous fluid supplementation. Although several strategies

such as antibodies against toxin, toxin binders, and Stx trafficking blockers are being tested at different levels [3], none of these have entered the clinical trials. Another potential prophylactic or therapeutic approach could be disruption or prevention of bacterial attachment to host surface.

Bacterial attachment to the host surface is mediated by a multitude of factors. Two key structures, namely flagella and locus of enterocyte effacement (LEE) help in colonization and attachment of EHEC to the epithelial cell surface [4,5]. Once ingested, EHEC traverses to large intestine by the guided flagellar motility [4] and attaches to the epithelial cell layer with the help of flagella, LEE and other surface structures such as type 1 pili and hemorrhagic coli pilus [6–8]. In the colon, a two component system involving Quorum Sensing *E. coli* Regulators (QseBC) regulates the expression of flagellar transcriptional regulators *flhDC* in response to the autoinducers (AI-2/AI-3) and endogenous hormones epinephrine (EPI), norepinephrine (NE) [5,9]. QseB, the response regulator directly binds to and induces expression of flagellar master regulators *flhD* and *flhC* [8].

Biofilm communities show better tolerance to antimicrobials and are a source of chronic infections [12]. Therefore, biofilm formation and/or attachment of EHEC to biotic/abiotic surfaces are considered potential targets for development of antimicrobials. Flagella are important regulators of biofilm formation in *E. coli* under natural settings and help in initial attachment and development of the complex community [10,11]. The importance of flagella in EHEC pathogenesis as well as in

* Corresponding author at: Vegetable and Fruit Improvement Center, Department of Horticulture Science, Ste A 120, 1500 Research Pkwy, College Station, TX 77845, USA. Tel.: +1 9798453864.

E-mail address: b-patil@tamu.edu (B.S. Patil).

biofilm formation makes it an attractive target for development of alternative intervention strategies. One potential strategy of intervention is identification of small molecules that target and inhibit biofilm formation and attachment.

Natural products are the end products of secondary metabolism in plants and microorganisms. They demonstrate diverse biological activities including antimicrobial properties [13]. By virtue of their diversity, natural products provide an excellent source for identification of novel molecules targeting bacterial virulence and pathogenesis. Numerous plant secondary metabolites with wide-ranging activities have been identified [13]. In our earlier studies, we identified several citrus limonoids and flavonoids that interfere with quorum sensing and virulence gene expression [14–17]. Additionally, the antimicrobial activity of citrus peel oils and extracts has been extensively reported [18,19]. However, the mechanism by which the essential oils exert their antimicrobial action is not completely understood [18]. Citrus peel is very complex matrix and contains many different classes of bioactive compounds including flavonoids, limonoids, carotenoids, coumarins, sterols and phenolic compounds [20]. We and others have reported diverse activities including bactericidal, bacteriostatic and anti-quorum sensing activity for some of the compounds present in citrus peel [14–16,21]. The present report describes the anti-virulence activities of coumarins, polymethoxyflavones and a phytosterol isolated from citrus on the biofilm formation and motility of the devastating pathogen EHEC.

2. Materials and methods

2.1. Isolation of bioactive compounds

Bergamottin [22], β -sitosterol glucoside (SG) [23], nobiletin, sinensetin [24], heptamethoxyflavone [25], and imperatorin [26] were purified in our lab. A 5 mM stock solution in DMSO was prepared and used for the studies. Briefly, clementine peel was dried, powdered and extracted with hexane using a Soxhlet type apparatus for 8 h. Vacuum concentrated hexane extract was separated over a silica gel (particle size 35–60 μ m) flash column on Teledyne Isco CombiFlash RF 4 \times system (Lincoln, NE). Compounds were eluted with increasing strength of acetone in hexane at a flow rate of 60 mL/min. The eluents were monitored at 340 nm. Three major peaks A, B and C were collected and vacuum dried to obtain three polymethoxyflavones (Supplementary Fig. S1). Further, β -sitosterol glucoside was purified by extracting defatted sour orange seed powder with ethyl acetate. The extract was dried under vacuum and separated on silica gel with 2:3 dichloromethane and acetone [23]. Bergamottin was purified by extracting grapefruit juice with ethyl acetate. The organic layer was concentrated under vacuum and purified on silica gel with increasing polarity of ethyl acetate in hexane. Fractions showing furcoumarin spot on TLC were pooled and further separated using Waters preparative HPLC system (Waters Corporation, Milford, Massachusetts, USA). Elution was carried out by increasing strength of methanol in water in gradient fashion [22]. Fractions containing bergamottin were pooled, concentrated and crystallized to obtain >95% pure bergamottin. Imperatorin was isolated from *Poncirus trifoliata*. The edible part of trifoliata oranges was freeze dried and extracted with chloroform. The vacuum dried extract was then separated on silica gel using flash chromatography to obtain imperatorin [26].

The compounds were identified by ultra-high performance liquid chromatography-time of flight-mass spectrometry (LC-QTOF-MS) (maXis impact, Bruker Daltonics, Billerica, MA). Isolated compounds were separated on a Kinetex C18 column (1.7 μ m, 100 \times 2.1 mm; Phenomenex, Torrance, CA, USA) using an Agilent 1290 UHPLC instrument (Agilent, Santa Clara, CA). The separation was carried out at 50 $^{\circ}$ C with a flow rate of 0.2 mL/min using gradient elution of 0.1% formic acid and acetonitrile. Mass spectral analyses were performed using the ESI-Q-TOF mass spectrometer equipped with an electrospray ionization source in positive ion mode. Capillary voltage was maintained

at 2.9 kV, source temperature was set at 200 $^{\circ}$ C and nitrogen was used as the desolvation gas (12 L/min).

2.2. Bacterial strains, media and samples

Bacterial strains used in this study are listed in Table 1. Unless otherwise specified, bacterial cultures were grown at 37 $^{\circ}$ C in Luria–Bertani (LB) medium. When appropriate, the medium was supplemented with chloramphenicol 10 μ g/ml and/or 0.2% arabinose.

2.3. Plasmids

A list of plasmids used in the study is presented in Table 1. All genetic manipulations were done as previously described [27]. The primers were designed by altering one base to create restriction sites. Total genomic DNA from EHEC was purified using CTAB method [27]. Expression plasmids were constructed by amplifying genomic DNA for each gene using primer pairs listed in Table 2 and Deep VentR DNA polymerase (New England Biolabs, Ipswich, MA). For *flhD*, a fragment of 623 bp starting at 125 bp upstream to 138 bp downstream at 3' end was amplified. The fragment was digested with *SacI* and *HindIII* and cloned into pBAD33 generating plasmid pAV13. *flhC* was amplified as 717 bp fragment starting at –103 to +614 bp, digested with *SacI* and *PstI* and cloned into pBAD33 generating plasmid pAV14. To generate plasmid pAV15, a fragment of 1099 bp was amplified using *flhD*-F and *flhC*-R primers, digested with *SacI* and *PstI* and cloned in pBAD33. For *fliA* a 960 bp fragment from –128 to +782 was amplified, digested with *SacI* and *PstI* and cloned into pBAD33 to generate plasmid pAV16. *ompR* was amplified as a fragment of 983 bp from –68 to +815, digested with *SacI* and *PstI* and cloned into pBAD33 generating plasmid pAV18. *envZ* was cloned into pBAD3 as a fragment of 1.72 kb from –170 to +1559 digested with *SmaI* and *HindIII*, giving rise to plasmid pAV17. A

Table 1
Bacterial Strains and plasmids used in the study.

Strain/Plasmid	Genotype	Reference/Source
<i>Strain</i>		
<i>E. coli</i> O157:H7 EDL933	Wild type	ATCC (#43895)
TEVS232	<i>LEE1:lacZ</i>	[29]
VS138	EHEC 86-24 <i>qseC</i> mutant	[9]
VS179	VS138 with plasmid pVS178 harboring <i>qseBC</i>	[9]
AV43	EHEC with plasmid pVS178	[17]
AV48	EHEC with plasmid pAV11	[17]
AV49	EHEC with plasmid pAV12	[17]
AV61	EHEC with plasmid pAV13	This study
AV64	EHEC with plasmid pAV15	This study
AV70	EHEC with plasmid pAV16	This study
AV75	EHEC with plasmid pAV18	This study
AV84	EHEC with plasmid pAV14	This study
AV81	EHEC with plasmid pAV19	This study
AV89	EHEC with plasmid pAV17	This study
AV90	EHEC with plasmid pAV20	This study
AV94	EHEC with plasmid pAV21	This study
AV100	EHEC with plasmid pAV22	This study
<i>Plasmids</i>		
pBAD33	Low copy expression vector	ATCC
pVS178	<i>E. coli</i> K12 <i>qseBC</i> in pBAD33	[9]
pAV11	EHEC <i>qseC</i> in pBAD33	[17]
pAV12	EHEC <i>qseB</i> in pBAD33	[17]
pAV13	EHEC <i>flhD</i> in pBAD33	This study
pAV14	EHEC <i>flhC</i> in pBAD33	This study
pAV15	EHEC <i>flhDC</i> in pBAD33	This study
pAV16	EHEC <i>fliA</i> in pBAD33	This study
pAV17	EHEC <i>envZ</i> in pBAD33	This study
pAV18	EHEC <i>ompR</i> in pBAD33	This study
pAV19	EHEC <i>ompR-envZ</i> in pBAD33	This study
pAV20	EHEC <i>rrsAB</i> in pBAD33	This Study
pAV21	EHEC <i>hns</i> in pBAD33	This Study
pAV22	EHEC <i>grpE</i> in pBAD33	This Study

Table 2
List of primers used in this study.

Gene	Orientation	Sequence	Restriction site	Reference
<i>qPCR primers</i>				
<i>flhC</i>	F	CGCTTCCAGCATCTGCAA		[15]
<i>flhC</i>	R	CGGATATTCAGCTGGCAAT		
<i>flhD</i>	F	TCATTCCAGCAAGCGTGTGAG		[15]
<i>flhD</i>	R	TCCCGCGTTGACGATCTC		
<i>rpoA</i>	F	GTTGCCGACGACGAATCGC		[15]
<i>rpoA</i>	R	CCCAATCGCCCTCTGCTGG		
<i>Cloning Primers</i>				
<i>flhD</i>	F	AAAAGGTGAGCTCTGCTTAT	SacI	This study
<i>flhD</i>	R	TCTTTATAAAGCTTTATCAGGC	HindIII	This study
<i>flhC</i>	F	TTGACGAGCTCCAGCAA	SacI	This study
<i>flhC</i>	R	TTACCGCTGCAGGAATGT	PstI	This study
<i>fliA</i>	F	GCAACATAGAGCTCAATTTG	SacI	This study
<i>fliA</i>	R	AGGTGCTGCAGCATCATT	PstI	This study
<i>ompR</i>	F	GACGAACGTGAGCTCTTTAAGA	SacI	This study
<i>ompR</i>	R	CCGTCCGTCAGTTGCAGT	PstI	This study
<i>envZ</i>	F	GCTCTCCCGGATAAGCT	SmaI	This study
<i>envZ</i>	R	AACACCTAAGCTTCCCGG	HindIII	This study
<i>rssAB</i>	F	TAATCTCCCGGAAACAATAACGG	SmaI	This study
<i>rssAB</i>	R	GGCTTTCGTCACGGCAACA	Sall	This study
<i>hns</i>	F	TTTAACCTCCCGGCTGCGAAAT	SmaI	This study
<i>hns</i>	R	CACGGAATTTAAAGCTTGGCTTGAAG	HindIII	This study
<i>grpE</i>	F	GCTCAACGATGAGCTCGTAACT	SacI	This study
<i>grpE</i>	R	ATTCGCCTGCAGGGCCGTGA	PstI	This study

fragment of 2.34 kb amplified using *ompR*-F and *envZ*-R primers, digested with SacI and HindIII and inserted into pBAD33 generating plasmid pAV19. *rssAB* in *E. coli* O157:H7 str. EDL933 was identified by homology to *rssB* and *rssA* gene sequences from *E. coli* O157:H7 str. TW14359 using BLAST search. The open reading frame (ORF) corresponding to *hnr* in Str. EDL933 showed 100% identity to *rssB* from Str. TW14359. Similarly, the upstream ORF *yckK*, showed 100% identity to *rssA*. Moreover, the genomic arrangement of *yckK* and *hnr* is similar to *rssA* and *rssB*. The intergenic region between *yckK* and *hnr* was 92 bp in Str. EDL933 compared to 110 bp in Str. TW14359. This analysis suggested that *yckK/hnr* are homologs of *rssA/rssB* and thus were used in the analysis. The 3.05 kb region encompassing the *yckK-hnr* ORFs was amplified with primer pair *rssAB*-F and *rssB*-R and digested with SmaI and Sall and cloned into pBAD33 generating plasmid pAV20. *hns* gene was amplified as a fragment of 812 bp from –206 to +606, digested with SmaI and HindIII and cloned into pBAD33 giving rise to plasmid pAV21. The heat shock protein *grpE* was amplified as 876 bp fragment from –243 to +633, digested with SacI and PstI and cloned into pBAD33 generating plasmid pAV22. All the plasmids were electroporated and maintained in *E. coli* K12 substr. DH10B and selected on LB-Agar plates containing 10 µg/ml of chloramphenicol. Colonies were picked up and screened for fragment insertion by PCR using the primers used for cloning. One positive clone for each was selected and maintained as freezer glycerol stock at –80 °C. Each plasmid was electroporated into the EHEC str. EDL933 to generate strains as listed in Table 1.

2.4. Growth activity

Overnight cultures of EHEC were diluted 100 fold in fresh LB media and grown aerobically at 37 °C for 16 h in the presence of 100 µM test compounds or the equivalent volume of DMSO as previously described [16]. A_{600} was recorded every 15 min using the Synergy™ HT Multi-Mode Microplate Reader (BioTek, Instruments, Winooski, VT). The data are presented as the mean of three biological replicates.

2.5. Biofilm assay

Biofilm assays were conducted as described [15]. Briefly, overnight cultures of *E. coli* O157:H7 strain ATCC 43895 were diluted 10 fold in LB or M63 and inoculated in presence of 3.125, 6.25, 12.5, 50, or

100 µM of each test compounds or the equivalent amount of DMSO in polystyrene 96-well plates at 26 °C for 24 h (48 h in case of VS138 and VS179) without shaking. Biofilm was quantified by staining with 0.3% crystal violet (Fisher, Hanover Park, IL) for 20 min. The inhibition of biofilm formation was calculated as $100 - [(OD_{570} \text{ of sample well} / OD_{570} \text{ of positive control}) \times 100]$ and expressed as percentage and SD values.

2.6. Motility assay

Motility assays were performed as described earlier [28]. Briefly diluted overnight cultures of EHEC were inoculated with sterile toothpick in the center of 0.3% LB-agar plates containing 100 µM test compounds or DMSO and incubated at 37 °C. Motility halos were measured after 12 and 24 h. The average of five replicated plates inoculated on different days is presented as mean ± SD.

2.7. Quantitative PCR

Relative transcript levels of *flhDC* (Table 2) were measured by qRT-PCR as previously described [15]. Briefly, overnight cultures of EHEC and EHEC overexpressing *flhD* (AV61), *flhC* (AV84), *flhDC* (AV64), *envZ* (AV89), *ompR* (AV75), *ompR-envZ* (AV81), *fliA* (AV70), *rssAB* (AV90), *hns* (AV94) and *grpE* (AV100) were diluted 100 fold with fresh LB medium containing 100 µM SG or DMSO and grown aerobically to $OD_{600} \approx 1.0$ at 37 °C. RNA was extracted using TRIzol (Life Technologies Corporation, Carlsbad, CA). The cDNA was synthesized using MuLV reverse transcriptase enzyme and random hexamer [27] and purified with QIAquick PCR-purification kit (Qiagen Inc.). Twenty five nanograms of cDNA was amplified with 10 pmol target primers using SYBR Green PCR master mix (Life Technologies Corporation, Carlsbad, CA) for 35 amplification cycles on an ABI-Prism 7000 HT (Applied Biosystems, Foster City, CA). Dissociation curves were generated to check the specificity of the PCR amplification. The C_t values for primers were normalized against that of 16S rRNA. Fold change in the gene expression was calculated by $2^{(-\Delta\Delta C_t)}$ and expressed as fold change ± SD of three replicates.

2.8. AI-3 reporter assay

Preconditioned medium (PM) was prepared as described [29]. Overnight culture of TEVS232 was diluted 100 fold in LB medium and grown

to OD₆₀₀ ≈ 0.2. The cells were collected by centrifugation at 2500 ×g for 10 min and resuspended in either fresh LB media supplemented with 50 μM epinephrine or PM and treated with 100 μM test compounds or equivalent volume of DMSO. The β-galactosidase activity was measured after 30 min incubation at 37 °C using *o*-nitrophenyl β-D-galactopyranoside and reported as mean ± SD of three replicates.

2.9. Statistical analysis

The effects of different compounds for each activity were analyzed with an analysis of variance (ANOVA) followed by Tukey's pairwise multiple comparison test on SPSS 16.0 (SPSS Inc., Chicago, IL, USA). The effect was considered significant at *p* < 0.05. For gene expression analysis the deviations from hypothetical value of 1.0 fold (no change) was calculated using SPSS 16.0.

3. Results

3.1. Identification of bioactive compounds

The isolated six compounds were identified by LC-MS with high resolution accurate mass spectral data. Fig. 1 shows the ESI-TOF mass spectra of the purified compounds from citrus. The compounds were identified by their high resolution accurate TOF-MS/MS data as heptamethoxy flavone 433.1508 [M + H]⁺, nobiletin 403.1386 [M + H]⁺, sinensitin 373.3735 [M + H]⁺, β-sitosterol glucoside 599.4257 [M + Na]⁺, bergamottin 339.3931 [M + H]⁺, and imperatorin 271.0991 [M + H]⁺.

599.4257 [M + Na]⁺, bergamottin 339.3931 [M + H]⁺, and imperatorin 271.0991 [M + H]⁺.

3.2. Effect of citrus bioactives on EHEC growth and biofilm formation

The EHEC biofilms were grown in rich and minimal medium and inhibition by different bioactive compounds was recorded at six concentrations ranging from 3.125 to 100 μM. The most potent inhibitor of EHEC biofilm formation under the both conditions was SG, followed by heptamethoxyflavone (Fig. 2A and B). To determine the IC₅₀ values, the data was fitted to 3-parameter model $y = a / (1 + \exp(-(x - x_0) / b))$ using SIGMAPLOT 11.0 (Systat Software, Inc.) and IC₅₀ values were calculated from the resulting equation. The IC₅₀ values for SG in LB and M63 were calculated as 8.3 and 13.9 μM respectively. The calculated IC₅₀ values for heptamethoxyflavone were 23.9 and 48.0 μM in LB and M63 respectively.

The growth of EHEC was measured to determine the effect of test compounds on the EHEC viability. The results demonstrate that the test compounds did not affect the growth of EHEC under the experimental conditions (Fig. 2C).

3.3. Effect on EHEC motility

To determine the effect of test compounds on motility, overnight cultures of EHEC were stabbed in the middle of 0.3% LB-agar plates prepared with 100 μM of each compound. Zone diameters were recorded after 12 and 24 h. All the tested compounds demonstrated significant

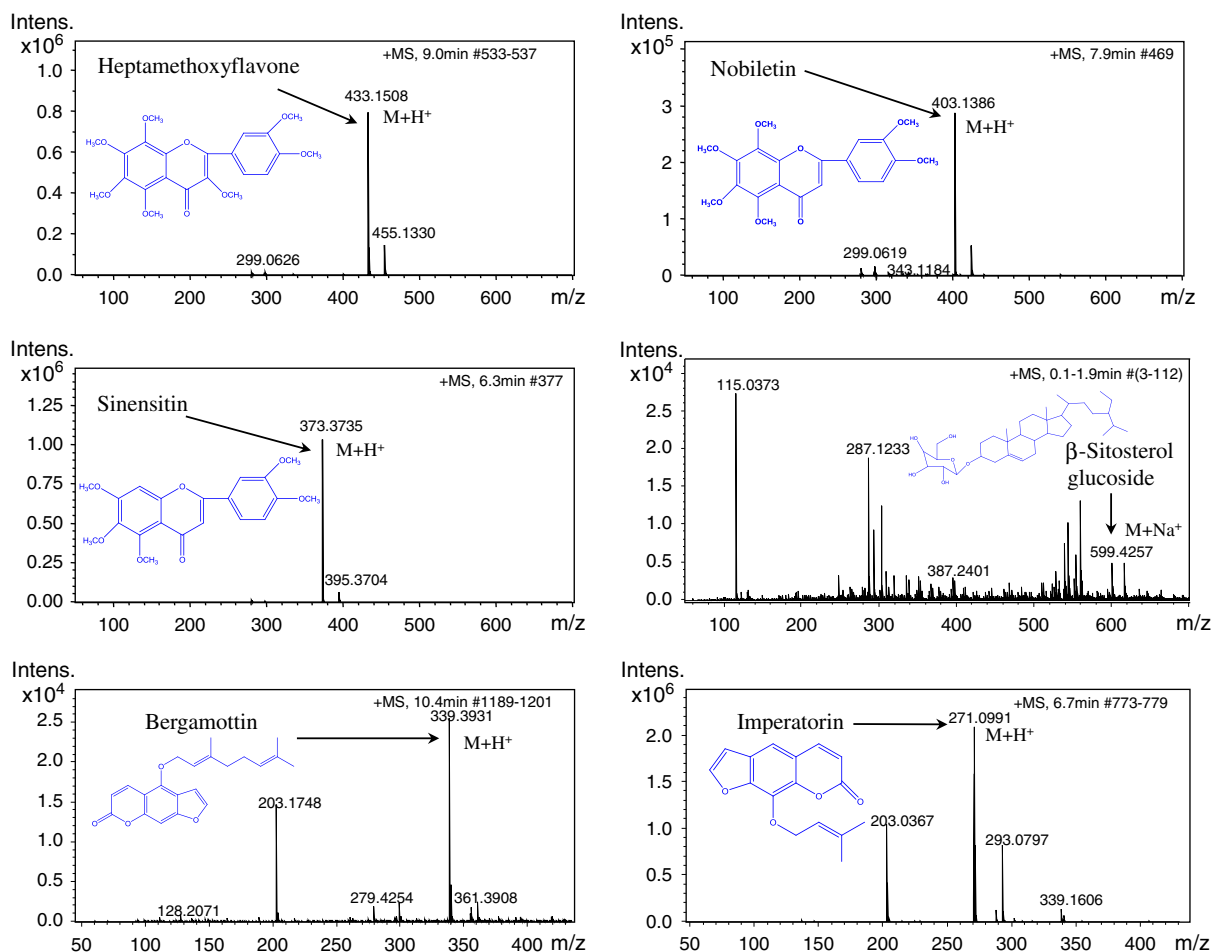


Fig. 1. Mass spectra of isolated bioactive compounds identified by accurate mass liquid chromatography/tandem mass spectrometry (LC/MS/MS) on a quadrupole time-of-flight (QTOF) by positive electrospray ionization (ESI) mode.

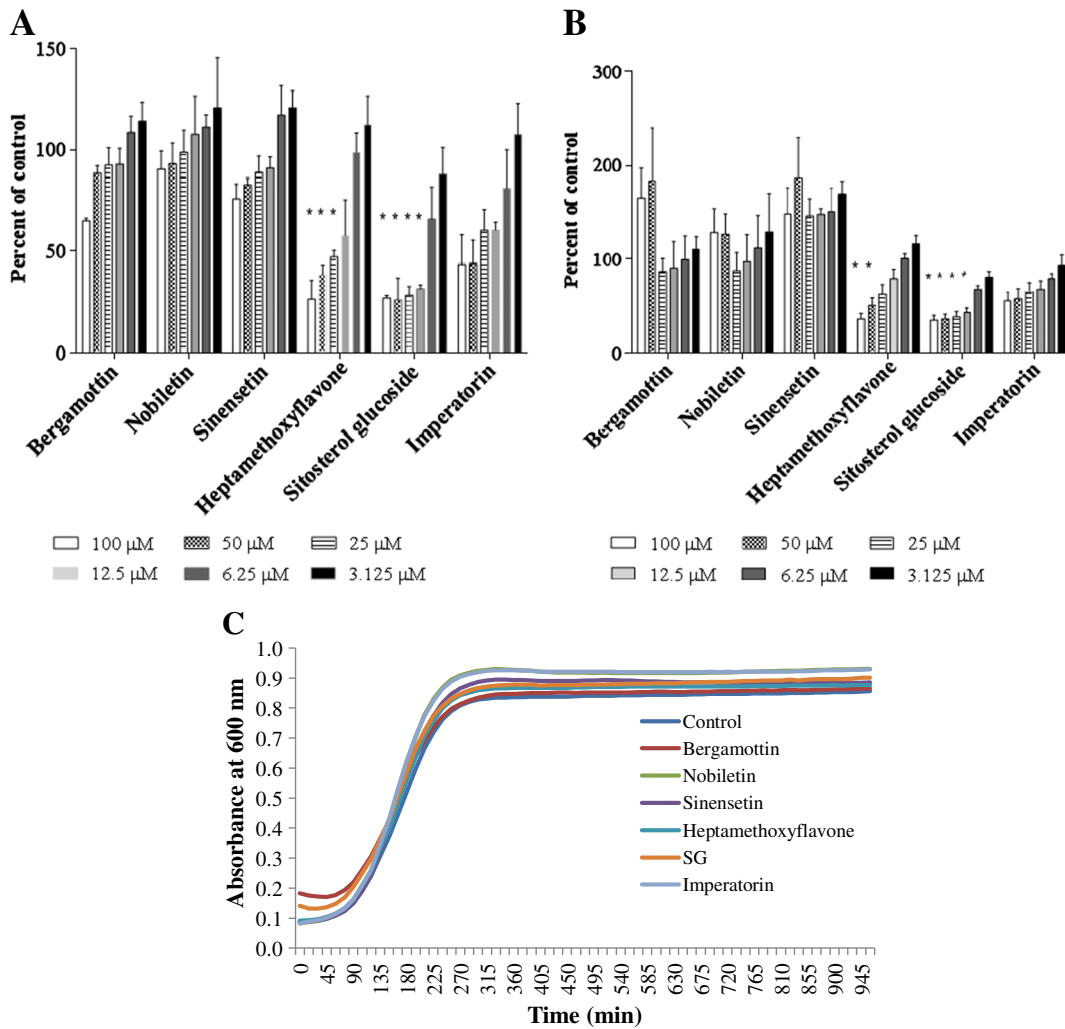


Fig. 2. EHEC biofilm formation in (A) rich (LB), and (B) minimal (M63) medium, in presence of citrus bioactive compounds. (C) Growth curves of EHEC in presence of 100 μM test compounds.

($p < 0.05$) inhibition the motility halos of EHEC (Fig. 3). SG was the most potent inhibitor and completely inhibited the motility of the EHEC. Even after 24 h the EHEC demonstrated a motility halo of only 0.4 cm compared to 6.73 cm halo of control (Fig. 3). The zone diameters for different compounds in ascending orders were SG < nobiletin < imperatorin < sinensetin < heptamethoxyflavone < bergamottin < DMSO at 12 h and SG < nobiletin < imperatorin < sinensetin < bergamottin < heptamethoxyflavone < DMSO at 24 h (Fig. 3), respectively.

3.4. Effect on AI-3/epinephrine mediated cell–cell signaling

Cell-cell signaling regulates biofilm and motility [9,30]; therefore, we first tested the possibility that test compounds interfere with cell–cell signaling. Interference with cell–cell signaling was determined using the reporter strain TEVS231 [29], which carries a chromosomal fusion *LEE1:lacZ* and responds to external AI-3 and epinephrine. The expression of *LEE1* was induced by suspending the cells in PM for 30 min and β -galactosidase activity was measured. Significant ($p < 0.05$) β -galactosidase activity was recorded in cells incubated in PM after 30 min compared to cells incubated in fresh LB media (data not shown). To measure the interference, the test compounds were added to the PM, which was used to suspend the cells, and β -galactosidase activity was measured after 30 min. SG demonstrated significant ($p < 0.01$) repression (≈ 2.8 fold) of β -galactosidase activity (Fig. 4A), while β -galactosidase activity for cultures treated with other compounds was similar to DMSO. Interference with epinephrine signaling was

measured in a similar fashion by adding 50 μM epinephrine in PM and 100 μM SG. The β -galactosidase activity for SG was similar to DMSO, indicating that SG did not affect epinephrine induced cell–cell signaling (Fig. 4B). Collectively, SG appears to interfere with AI-3 but seems not to affect epinephrine induced activity. Other test compounds do not seem to interfere with AI-3 or epinephrine mediated cell–cell signaling. We further measured the expression of *stx2* gene using qPCR to determine the stress response. The relative expression of *stx2* was 1.6 (± 0.12) fold suggesting no adverse effect on the cell.

3.5. SG inhibits EHEC biofilm by repressing *flhDC*

Interference with AI-3 signaling and motility/biofilm formation by SG, suggested a possible effect on flagella as it is an important contributory factor in biofilm and motility. To determine the effect on flagella, expression of *flhDC* was measured using qRT-PCR. SG treatment repressed the expression of *flhC* and *flhD* by ≈ 6 and 7 folds, respectively (Fig. 5A). To further understand the effect of SG, the master regulators *flhD* (AV61), *flhC* (AV84), and *flhDC* (AV64) were induced with 0.2% arabinose and biofilm formation in presence of 100 μM SG or DMSO were compared after 24 h. Overexpression of either *flhD*, *flhC* or *flhDC* allowed similar levels of biofilm formation in presence of the SG or DMSO ($p > 0.05$) (Fig. 5B). Together, these results indicated that SG exerts a repressive effect on *flhDC*, and possibly modulates biofilm and motility in an *flhDC* dependent manner.

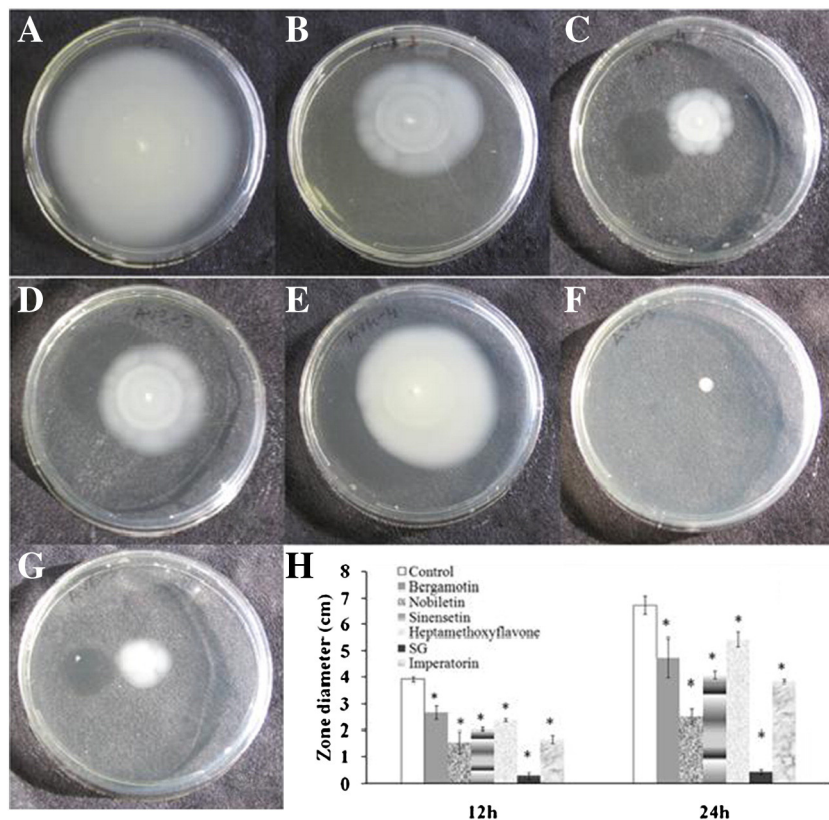


Fig. 3. Representative images of EHEC motility at 24 h in presence of 100 μ M (A) DMSO, (B) bergamotin, (C) nobiletin, (D) sinenstin, (E) heptamethoxyflavone, (F) SG and (G) imperatorin. Mean zone diameter (calculated from five replicates) for various treatments are presented in (H). Star denotes significant difference at $p < 0.01$.

3.6. The biofilm inhibition by SG is not mediated by *qseBC*, *envZ/ompR* or *fliA*

Interference with AI-3 mediated cell–cell signaling and repression of flagellar master regulators *flhDC* indicated a potential involvement of *qseBC* [31]. To determine the involvement of *qseBC* in SG-mediated repression of *flhDC* and biofilm formation, biofilm formation in strains Δ *qseC* (VS138) and *qseBC* complemented strain VS179 was measured.

VS138 is a *qseC* mutant, where *qseC* gene is replaced with gene encoding tetracycline [9]. It was expected that in the absence of functional *qseBC*, SG would not inhibit the EHEC biofilm. Indeed, the biofilm formation in the Δ *qseC* strain was similar in the presence of DMSO and SG (Fig. 6A), whereas a significant inhibition of biofilm formation by SG was observed in complemented strain VS179. In order to further understand the effect of SG, *qseBC* (AV43), *qseC* (AV48) and *qseB* (AV49) were overexpressed and biofilm formation was measured in presence of 100 μ M SG. SG

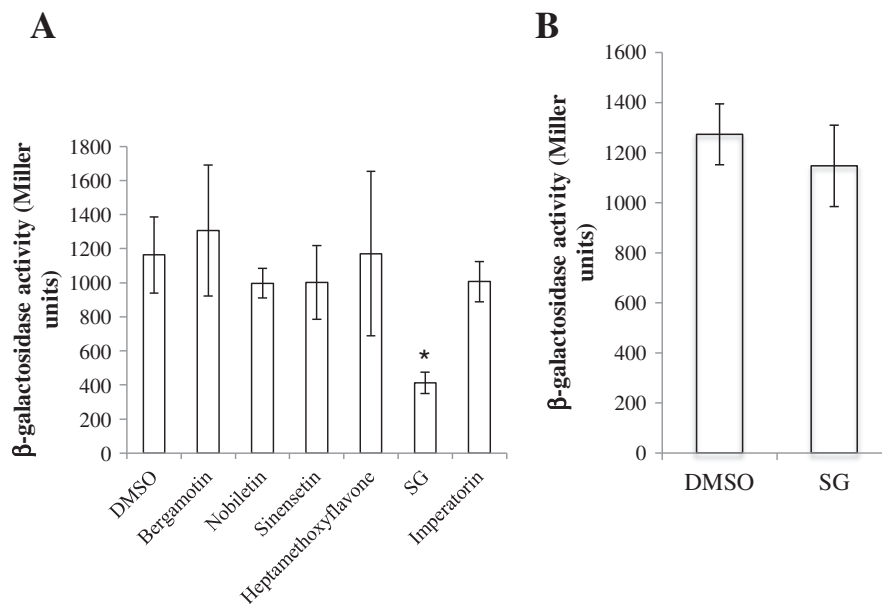


Fig. 4. (A) Effect of 100 μ M test compounds on *LEE1:lacZ* β -galactosidase activity, induced with Preconditioned Medium. (B) Effect of 100 μ M SG on epinephrine (50 μ M) induced *LEE1:lacZ* β -galactosidase activity. Star denotes significant difference at $p < 0.01$.

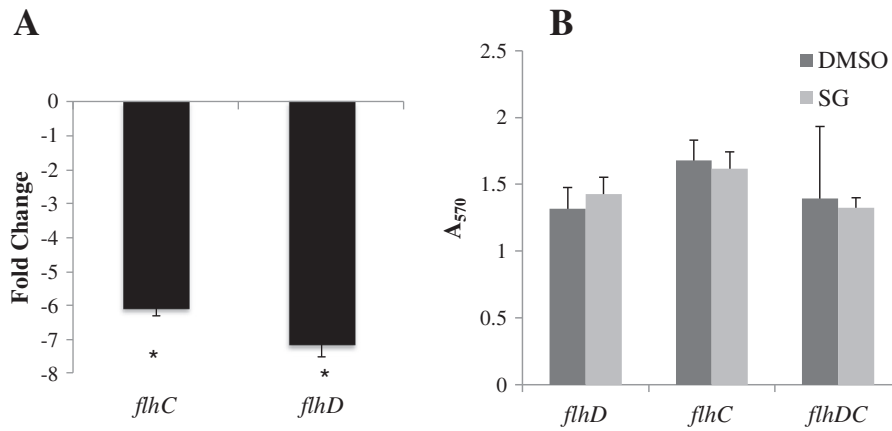


Fig. 5. (A) Expression of *flhDC* in EHEC upon exposure to 100 μ M SG. (B) Effect of SG on EHEC biofilm overexpressing *flhD* (AV61), *flhC* (AV84) and *flhDC* (AV64). Star denotes significance at $p < 0.01$.

demonstrated significant ($p < 0.01$) inhibition of biofilms formed by the three strains (Fig. 6B), suggesting that action of SG is not dependent upon *qseBC*.

In addition to *QseBC*, *EnvZ/OmpR* and *FliA* are also reported to regulate *flhDC* [31,32]. The role of *EnvZ/OmpR* and *FliA* was investigated by over-expressing the three genes from an arabinose controlled promoter in vector *pBAD33*. It was postulated that if inhibition of biofilm formation and *flhDC* by SG is mediated through *EnvZ/OmpR* or *FliA*, over-expression of the corresponding gene will relieve the inhibitory effect of SG. However, SG significantly ($p < 0.05$) inhibited the biofilms formed by the strains overexpressing *envZ* (AV89), *ompR* (AV75), *ompR-envZ* (81) and *fliA* (AV70) (Fig. 7A). Furthermore, *flhDC* was repressed ≈ 3.6 to 4.5 fold by 100 μ M SG in strains overexpressing *envZ*, *ompR*, *ompR-envZ* and *fliA* (Fig. 7B). These results indicate that SG inhibition of EHEC biofilm formation and *flhDC* does not require *EnvZ/OmpR* or *FliA*.

3.7. Overexpression of *hns* and *rssAB* rescues the EHEC biofilm and motility

Since overexpression of *qseBC*, *envZ/ompR* and *fliA* failed to rescue the biofilm inhibition and expression of *flhDC*, we next investigated the role of three additional positive regulators *grpE*, *hns* and *rssAB* [33–35]. The three genes were overexpressed under the arabinose-controlled operon in *pBAD33* in EHEC background. Interestingly, overexpression of *hns* (AV94) and *rssAB* (AV90) resulted in higher biofilm levels in presence of SG compared to DMSO (Fig. 8A), but *grpE* (AV100) did not have an effect. Furthermore, expression of *flhDC* was induced 2.1 and 1.2 fold in AV90 (*rssAB*) and AV94 (*hns*) in the presence of 100 μ M SG. In contrast, *flhC* and *flhD* were repressed the by 3.3 and 6.1 fold, respectively in AV100 overexpressing *grpE* (Fig. 8B).

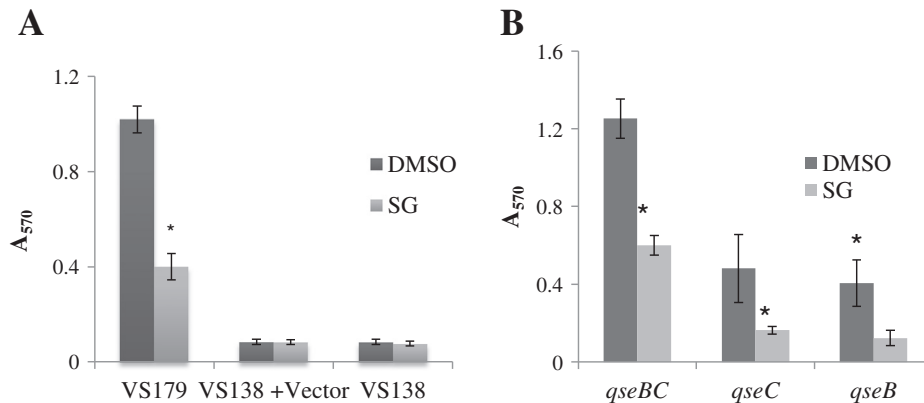


Fig. 6. Effect of SG on biofilm formation in (A) *qseC* mutant (VS138) and *qseC* mutant complemented with p^{qseBC} (VS179) and (B) EHEC overexpressing *qseBC* (AV43), *qseC* (AV48) and *qseB* (AV49). Star denotes significant difference at $p < 0.01$.

To further confirm these results, we measured the motility of strains overexpressing *hns* and *rssAB* (AV94 and AV90, respectively) in presence of 100 μ M SG. The measurements were recorded at 6.5 h to avoid the overlapping of the motility zones. The results demonstrated that *hns* and *rssAB* rescued the inhibition of the motility (Fig. 8C and D), and motility halos were comparable to that of strain AV64, overexpressing *flhDC*. Together, these results indicate that SG exerts its effect on EHEC biofilm formation and motility in an *hns* and *rssAB* dependent manner.

4. Discussion

The present study investigated the effect of secondary metabolites present in citrus on EHEC biofilm and motility. The flavedo is the outermost part of citrus fruit and provide defense against biotic and abiotic stress [36]. To aid in its function, the flavedo contains numerous structural adaptations and protective chemical constituents. The bioactive compounds present in flavedo or produced in oil glands, such as β -sitosterol, polymethoxyflavones and coumarins, are speculated to aid in defense against biotic stress such as by deterring bacterial pathogens. It is likely that these bioactive compounds may also demonstrate biological activity against human pathogens. To test this hypothesis, we evaluated the effect of six phytochemicals isolated from citrus peel on EHEC biofilm formation and motility.

The microtiter plate assay method, which non-specifically measures the early events in biofilm formation and attachment/adherence of bacterium to plastic surface was used to determine the effect of test compounds. This method has the advantage of being high throughput and mimics the early developmental stages of biofilm [37]. The experiment was conducted under nutrient rich and minimal media conditions

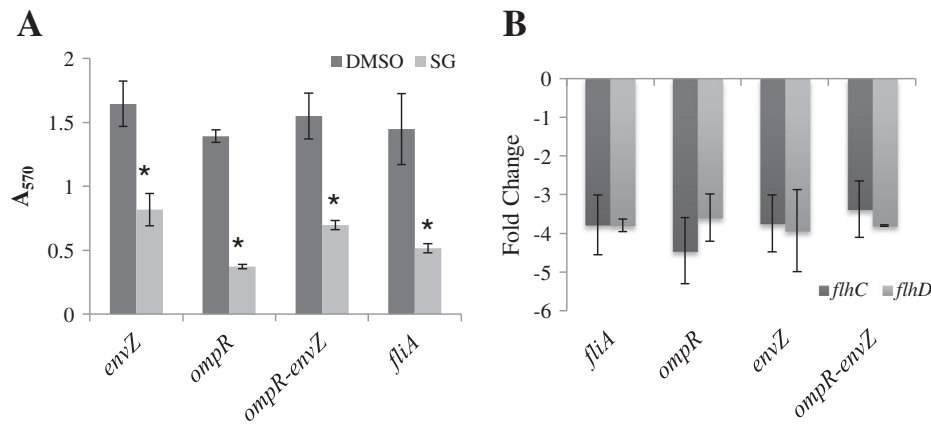


Fig. 7. (A) Effect of SG on (A) EHEC biofilm formation and (B) expression of *flhDC* in EHEC overexpressing *envZ* (AV89), *ompR* (AV75), *ompR-envZ* (AV81) and *flhA* (AV70). Star denotes significant difference at $p < 0.05$.

as *E. coli* produces different appendages for attachment under the two conditions. Different compounds demonstrated varying degree of inhibition under the two experimental conditions (Fig. 2). The SG appeared to be the most potent inhibitor of the EHEC biofilm (Fig. 2) and motility (Fig. 3) among the tested compounds under experimental conditions. Furthermore, the effect of SG and other compounds do not seem to be due to toxicity at tested concentrations.

AI-2/AI-3/epinephrine mediated cell-cell signaling regulates biofilm formation and motility in EHEC [9]. Inhibition of both biofilm formation and motility indicated the possibility that the tested compounds interfere with cell–cell signaling. Interference with AI-3/epinephrine mediated signaling was determined using reporter strain TEVS232, induced by PM or epinephrine. SG inhibited AI-3 mediated induction of LEE1 but

was ineffective against epinephrine (Fig. 4). Epinephrine is a mammalian hormone and is thus unlikely to be present on the plant surfaces. As secondary metabolites might have evolved to counter the endogenous molecules and associated signaling pathways of microbes, it is possible that SG selectively inhibit AI-3 signaling, and responds to AI-3 produced by natural microflora on citrus peels. Alternatively, it is possible that the SG targets a different pathway to inhibit biofilm and motility. Since SG was the most potent among the tested compounds, it was investigated to determine mechanism of action.

Flagella make an important contribution to EHEC biofilm and motility and are regulated by several genetic and environmental factors [9,32,33]. The flagellar master regulator *flhDC* regulates the transcriptional cascade of the flagellar operon and therefore, is the target of transcriptional

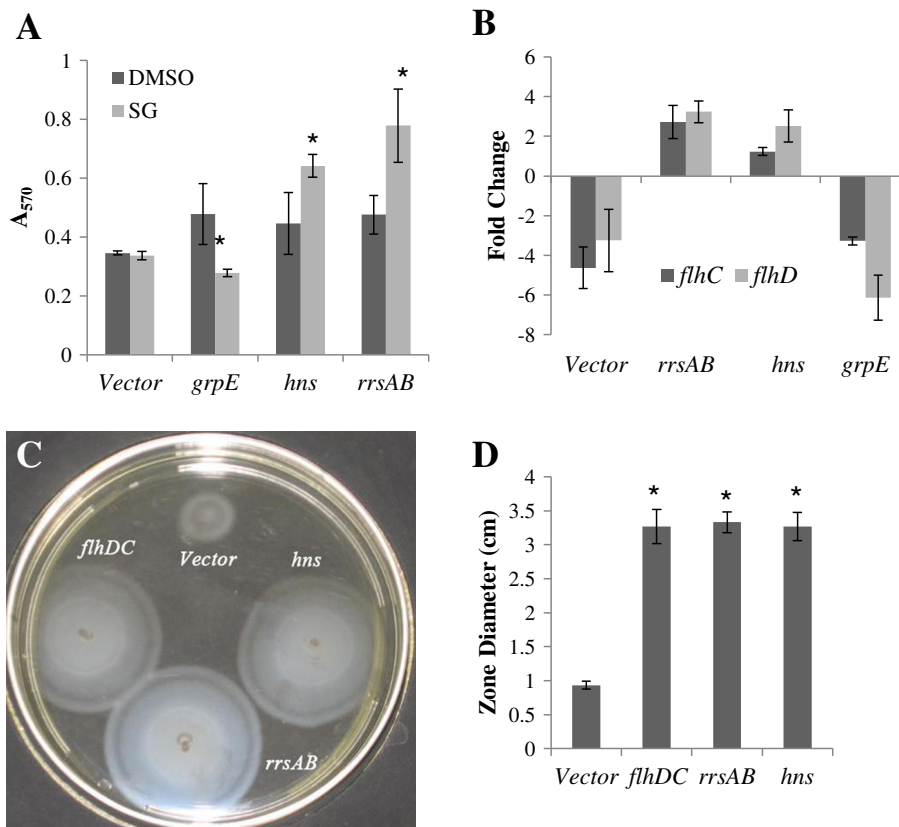


Fig. 8. Effect of SG on (A) EHEC biofilm formation and (B) expression of *flhDC* in EHEC overexpressing *rrsAB* (AV90), *hns* (AV94) and *grpE* (AV100). (C) Motility of EHEC strains overexpression of *flhDC* (AV64), *rrsAB* (AV90) and *hns* (AV94) on motility-agar plate containing 100 μ M SG. Representative figure is presented. (D) Zone diameters of AV64, AV94, AV100 and vector control in presence of 100 μ M SG.

regulation by various factors. We first determined if SG modulates the expression of *flhDC* using qRT-PCR. SG appears to repress *flhDC*. If SG function requires *flhDC*, overexpression of *flhDC* may negate the inhibition of biofilm formation caused by SG. Indeed, overexpression of both *flhD* and *flhC* relieved the inhibitory effect of SG on biofilm (Fig. 5A) and motility (Fig. 8C) in our assays, suggesting that the effect of SG is mediated by *flhDC*. Furthermore, transcriptional repression of *flhDC* indicated that SG regulates the flagellar operon (Fig. 5B), plausibly by acting on certain upstream factor/s.

QseBC is a two component systems, which regulates expression of *flhDC* in response to AI-3 and epinephrine [9]. Since SG seems to interfere with AI-3 signaling and repress *flhDC*, it was likely that SG function requires QseBC. Therefore, we examined the effect of SG on QseBC by using $\Delta qseC$ and *qseBC* complemented strains VS138 and VS179, respectively. In $\Delta qseC$, biofilm formation in the presence of SG was similar to DMSO. However, $\Delta qseC$ formed very little biofilm even after 48 h and it remained possible that the observed phenotype was due to *qseC* deletion and the effect of SG was not discernible. To further clarify, QseBC were overexpressed from an arabinose-controlled promoter in EHEC background. Overexpression of *qseBC* in EHEC background was expected to relieve the inhibitory effect of SG on EHEC biofilm formation. However, significant inhibition of the biofilm formation in EHEC overexpressing *qseBC* (AV43), *qseC* (AV48) and *qseB* (AV49) suggested that the effect of SG is not mediated through QseBC.

Several factors other than QseBC regulate *flhDC*. Some of the factors such as *empZ/ompR*, *rssAB*, *fliA*, *grpE* and *hns* positively regulate the expression of *flhDC* [32–35]. To determine the roles of the selected factors, each gene was over-expressed in EHEC background and biofilm formation in the presence of SG was measured. The hypothesis was that over-expression of the SG-target gene will rescue the biofilm formation. Overexpression of *empZ/ompR*, *fliA* and *grpE* did not alter the inhibitory effect of SG on biofilm and *flhDC* expression but over-expression of *hns* and *rssAB* rescued biofilm formation and motility by restoring *flhDC* expression (Fig. 8C). Intriguingly, we observed a higher level of biofilm formation in the presence of SG in strains overexpressing *hns* and *rssAB*. However, the implications of this observation are not clear as of yet and require further studies.

RssAB is a two component system that senses environmental signals such as temperature and exogenous fatty acids and regulates swarming [38]. In biological system, SG may convert to sitosterol and glucose molecule, the lipophilic sitosterol may function through *rssAB* to repress swarming in a similar fashion to saturated fatty acids. In summary, SG appears to inhibit the EHEC biofilm and motility by repressing *flhDC* via a mechanism involving *hns* and *rssAB*. Further work will be required to clearly determine the target/s of SG and its potential use as a lead molecule in developing novel antivirulence strategies. Another possible advantage of using SG as anti-virulence agent may lie in its other beneficial properties, which include cholesterol lowering and immunomodulatory activities.

Supplementary data to this article can be found online at <http://dx.doi.org/10.1016/j.bbagen.2013.07.022>.

Acknowledgements

We would like to thank Dr. V. Sperandio (University of Texas Southwestern Medical Center, Dallas, TX) for generously providing AI-3 reporter strains harboring chromosomal *LEE1:lacZ* (TEVS232), *LEE2:lacZ* (TEVS21) and EHEC mutants VS145, VS151, VS138, VS179. This project is based upon the work supported by the USDA-NIFA No. 2010-34402-20875, “Designing Foods for Health” through the Vegetable & Fruit Improvement Center.

References

- [1] A.E. Clatworthy, E. Pierson, D.T. Hung, Targeting virulence: a new paradigm for antimicrobial therapy, *Nat. Chem. Biol.* 3 (2007) 541–548.

- [2] J.B. Kaper, J.P. Nataro, H.L.T. Mobley, Pathogenic *Escherichia coli*, *Nat. Rev. Microbiol.* 2 (2004) 123–140.
- [3] P. Goldwater, K. Bettelheim, Treatment of enterohemorrhagic *Escherichia coli* (EHEC) infection and hemolytic uremic syndrome (HUS), *BMC Med.* 10 (2012) 12.
- [4] J.A. Girón, A.G. Torres, E. Freer, J.B. Kaper, The flagella of enteropathogenic *Escherichia coli* mediate adherence to epithelial cells, *Mol. Microbiol.* 44 (2002) 361–379.
- [5] A.R. Pacheco, V. Sperandio, Inter-kingdom signaling: chemical language between bacteria and host, *Curr. Opin. Microbiol.* 12 (2009) 192–198.
- [6] J. Xicohtencatl-Cortes, V. Monteiro-Neto, M.A. Ledesma, D.M. Jordan, O. Francetic, J.B. Kaper, J.L. Puentes, J.A. Girón, Intestinal adherence associated with type IV pili of enterohemorrhagic *Escherichia coli* O157:H7, *J. Clin. Investig.* 117 (2007) 3519–3529.
- [7] M.A. Rendon, Z. Saldana, A.L. Erdem, V. Monteiro-Neto, A. Vázquez, J.B. Kaper, J.L. Puentes, J.A. Girón, Commensal and pathogenic *Escherichia coli* use a common pilus adherence factor for epithelial cell colonization, *Proc. Natl. Acad. Sci.* 104 (2007) 10637–10642.
- [8] T. Bansal, D. Englert, J. Lee, M. Hegde, T.K. Wood, A. Jayaraman, Differential effects of epinephrine, norepinephrine, and indole on *Escherichia coli* O157:H7 chemotaxis, colonization, and gene Expression, *Infect. Immun.* 75 (2007) 4597–4607.
- [9] V. Sperandio, A.G. Torres, J.B. Kaper, Quorum sensing *Escherichia coli* regulators B and C (QseBC): a novel two-component regulatory system involved in the regulation of flagella and motility by quorum sensing in *E. coli*, *Mol. Microbiol.* 43 (2002) 809–821.
- [10] T. Wood, A. González Barrios, M. Herzberg, J. Lee, Motility influences biofilm architecture in *Escherichia coli*, *Appl. Microbiol. Biotechnol.* 72 (2006) 361–367.
- [11] A. Reisner, K.A. Krogfelt, B.M. Klein, E.L. Zechner, S. Molin, In vitro biofilm formation of commensal and pathogenic *Escherichia coli* strains: Impact of environmental and genetic factors, *J. Bacteriol.* 188 (2006) 3572–3581.
- [12] J.W. Costerton, P.S. Stewart, E.P. Greenberg, Bacterial biofilms: a common cause of persistent infections, *Science* 284 (1999) 1318–1322.
- [13] M.M. Cowan, Plant products as antimicrobial agents, *Clin. Microbiol. Rev.* 12 (1999) 564–582.
- [14] A. Vikram, P.R. Jesudhasan, G.K. Jayaprakasha, S.D. Pillai, A. Jayaraman, B.S. Patil, Citrus flavonoid represses *Salmonella* pathogenicity island 1 and motility in *S. Typhimurium* LT2, *Int. J. Food Microbiol.* 145 (2011) 28–36.
- [15] A. Vikram, P.R. Jesudhasan, G.K. Jayaprakasha, S.D. Pillai, B.S. Patil, Grapefruit bioactive limonoids modulate *E. coli* O157:H7 TTSS and biofilm, *Int. J. Food Microbiol.* 140 (2010) 109–116.
- [16] A. Vikram, P.R. Jesudhasan, G.K. Jayaprakasha, S.D. Pillai, B.S. Patil, Citrus limonoids interfere with *Vibrio harveyi* cell–cell signaling and biofilm formation by modulating response regulator *luxO*, *Microbiology* 157 (2011) 99–110.
- [17] A. Vikram, P.R. Jesudhasan, S. Pillai, B. Patil, Isolimononic acid interferes with *Escherichia coli* O157:H7 biofilm and TTSS in QseBC and QseA dependent fashion, *BMC Microbiol.* 12 (2012) 261.
- [18] K. Fisher, C. Phillips, Potential antimicrobial uses of essential oils in food: is citrus the answer? *Trends Food Sci. Technol.* 19 (2008) 156–164.
- [19] T.R. Callaway, J.A. Carroll, J.D. Arthington, C. Pratt, T.S. Edrington, R.C. Anderson, M.L. Galeyan, S.C. Ricke, P. Crandall, D.J. Nisbet, Citrus products decrease growth of *E. coli* O157:H7 and *Salmonella* Typhimurium in pure culture and in fermentation with mixed ruminal microorganisms In vitro, *Foodborne Pathog. Dis.* 5 (2008) 621–627.
- [20] J.A. Manthey, K. Grohmann, Phenols in citrus peel byproducts. Concentrations of hydroxycinnamates and polymethoxylated flavones in citrus peel molasses, *J. Agric. Food Chem.* 49 (2001) 3268–3273.
- [21] T.P.T. Cushnie, A.J. Lamb, Antimicrobial activity of flavonoids, *Int. J. Antimicrob. Agents* 26 (2005) 343–356.
- [22] B. Girennavar, S.M. Poulse, G.K. Jayaprakasha, N.G. Bhat, B.S. Patil, Furocoumarins from grapefruit juice and their effect on human CYP 3A4 and CYP 1B1 isoenzymes, *Bioorg. Med. Chem.* 14 (2006) 2606–2612.
- [23] G.K. Jayaprakasha, Y. Jadegoud, G.A. Nagana Gowda, B.S. Patil, Bioactive compounds from sour orange inhibit colon cancer cell proliferation and induce cell cycle arrest, *J. Agric. Food Chem.* 58 (2009) 180–186.
- [24] R.M. Uckoo, G.K. Jayaprakasha, B.S. Patil, Rapid separation method of polymethoxyflavones from citrus using flash chromatography, *Sep. Purif. Technol.* 81 (2011) 151–158.
- [25] R.M. Uckoo, G.K. Jayaprakasha, B.S. Patil, Hyphenated flash chromatographic separation and isolation of furocoumarins and polymethoxyflavones from byproduct of citrus juice processing industry, *Sep. Sci. Technol.* 48 (2013) 1467–1472.
- [26] G.K. Jayaprakasha, K.N.C. Murthy, B.S. Patil, Inhibition of pancreatic cancer cells by furocoumarins from *Poncirus trifoliata*, *Planta Med.* 78 (2012) P1175.
- [27] J. Sambrook, D.W. Russell, *Molecular Cloning: A Laboratory Manual*, the third edition Cold Spring Harbor Laboratory Press, Cold Spring Harbor, New York, 2001.
- [28] P.R. Jesudhasan, M.L. Cepeda, K. Widmer, S.E. Dowd, K.A. Soni, M.E. Hume, J. Zhu, S.D. Pillai, Transcriptome analysis of genes controlled by *luxS/Autoinducer-2* in *Salmonella enterica* serovar Typhimurium, *Foodborne Pathog. Dis.* 7 (2010) 399–410.
- [29] V. Sperandio, J.L. Mellies, W. Nguyen, S. Shin, J.B. Kaper, Quorum sensing controls expression of the type III secretion gene transcription and protein secretion in enterohemorrhagic and enteropathogenic *Escherichia coli*, *Proc. Natl. Acad. Sci.* 96 (1999) 15196–15201.
- [30] A.F. Gonzalez Barrios, R. Zuo, Y. Hashimoto, L. Yang, W.E. Bentley, T.K. Wood, Autoinducer 2 controls biofilm formation in *Escherichia coli* through a novel motility quorum-sensing regulator (MqsR, B3022), *J. Bacteriol.* 188 (2006) 305–316.
- [31] M.B. Clarke, V. Sperandio, Transcriptional regulation of *flhDC* by QseBC and σ 28 (FlhA) in enterohaemorrhagic *Escherichia coli*, *Mol. Microbiol.* 57 (2005) 1734–1749.
- [32] Y. Hu, Y. Wang, L. Ding, P. Lu, S. Atkinson, S. Chen, Positive regulation of *flhDC* expression by *OmpR* in *Yersinia pseudotuberculosis*, *Microbiology* 155 (2009) 3622–3631.
- [33] O. Soutourina, A. Kolb, E. Krin, C. Laurent-Winter, S. Rimsky, A. Danchin, P. Bertin, Multiple control of flagellum biosynthesis in *Escherichia coli*: role of H-NS protein

- and the Cyclic AMP-catabolite activator protein complex in transcription of the *flhDC* master operon, *J. Bacteriol.* 181 (1999) 7500–7508.
- [34] W. Shi, Y. Zhou, J. Wild, J. Adler, C.A. Gross, DnaK, DnaJ, and GrpE are required for flagellum synthesis in *Escherichia coli*, *J. Bacteriol.* 174 (1992) 6256–6263.
- [35] P.-C. Soo, Y.-T. Horng, J.-R. Wei, J.-C. Shu, C.-C. Lu, H.-C. Lai, Regulation of swarming motility and *flhDC_{sm}* expression by RssAB signaling in *Serratia marcescens*, *J. Bacteriol.* 190 (2008) 2496–2504.
- [36] F.S. Davies, L.G. Albrigo, Citrus, CAB International, Wallingford, UK, 1994.
- [37] G. O'Toole, H.B. Kaplan, R. Kolter, Biofilm formation as microbial development, *Ann. Rev. Microbiol.* 54 (2000) 49–79.
- [38] H.-C. Lai, P.-C. Soo, J.-R. Wei, W.-C. Yi, S.-J. Liaw, Y.-T. Horng, S.-M. Lin, S.-W. Ho, S. Swift, P. Williams, The RssAB two-component signal transduction system in *Serratia marcescens* regulates swarming motility and cell envelope architecture in response to exogenous saturated fatty acids, *J. Bacteriol.* 187 (2005) 3407–3414.